

Uniform convergence of discrete curvatures from nets of curvature lines

Ulrich Bauer^{*} Konrad Polthier[†] Max Wardetzky^{*}

January 19, 2009

Abstract

We study “Steiner-type” discrete curvatures computed from nets of curvature lines on a given smooth surface, and prove their uniform pointwise convergence to smooth principal curvatures. We provide explicit error bounds, with constants depending only on the limit surface and the shape regularity of the discrete net.

1 Introduction

The field of *discrete differential geometry* has been revealing intriguing discrete counterparts to classical differential-geometric concepts as well as useful geometric algorithms (see, e.g., [Bobenko et al., 2008](#); [Grinspun and Desbrun, 2006](#)). One central aspect of this theory is *convergence*: classical smooth notions should arise in the limit of refinement of discrete ones. Recently, several convergence results have been obtained for curvatures and differential operators associated with polyhedral surfaces. Roughly, one may distinguish three different approaches of treating convergence: based on (i) polynomial surface approximation (see, e.g., [Meek and Walton, 2000](#); [Cazals and Pouget, 2005](#)), (ii) geometric measure theory (see, e.g., [Fu, 1993](#); [Cohen-Steiner and Morvan, 2006](#)), and (iii) finite element analysis (see, e.g., [Dziuk, 1988](#); [Hildebrandt et al., 2006](#)). Among these, (i) provides *pointwise* curvature estimates for many, but not all, discrete meshes. In contrast, the latter two approaches consider generalizations of *integrated*, or total, curvatures and yield convergence in the sense of measures or appropriate Sobolev norms, respectively. Assuming shape regularity, these latter two approaches apply to arbitrary polyhedral surfaces.

Given convergence in an *integrated* sense, it is natural to ask whether the discrete curvatures considered by (ii) and (iii) above can be shown to converge in a *pointwise* manner. In general, the answer to this question is negative: it was observed in [Xu et al. \(2005\)](#) that for general irregular polyhedral surfaces, there exists no *k-local* definition of discrete curvature that is pointwise convergent. Here, by *k-locality* we mean that

^{*}Institute for Numerical and Applied Mathematics, University of Göttingen, Lotzestr. 16–18, 37083 Göttingen, Germany. <http://ddg.math.uni-goettingen.de/>

[†]Department of Mathematics and Computer Science, Freie Universität Berlin, Arnimallee 6, 14195 Berlin, Germany. <http://geom.mi.fu-berlin.de/>

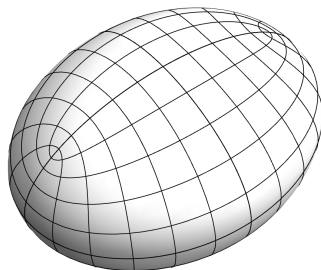


Figure 1: A discrete net of curvature lines of an ellipsoid.

the definition of the curvatures associated with each vertex p only depend on its k -star, i.e., those vertices that are connected to p by a path of at most k edges. The concept of k -locality is motivated by the smooth case, where curvatures and differential operators only depend on local properties of the underlying Riemannian manifold.

Pointwise convergence from nets of curvature lines We provide an affirmative answer to the above question of pointwise convergence for a *special class* of discrete meshes: discrete nets of curvature lines on a given surface immersed into \mathbb{E}^3 (see Figure 1). Using these nets, we consider 1-local definitions of discrete curvatures that are of “Steiner-type”, i.e., constructed using offsets (see Section 2.1 for precise statements). This encompasses discrete curvatures based on the theory of normal cycles (see, e.g., [Cohen-Steiner and Morvan, 2006](#)) as well as those based on linear finite elements (see, e.g., [Pinkall and Polthier, 1993](#)). For these schemes, we show *uniform pointwise convergence* of discrete curvatures to principal curvatures of the given smooth limit surface (see Theorem 1). Similarly, we prove uniform pointwise convergence of discrete mean curvatures. In order to guarantee uniformity, we make the constants in our estimates *explicit*. Specifically, our results hold up to, and including, umbilical points of discrete nets of curvature lines (see Figure 2).

Several convergence results for discrete mean curvatures and curvature-based energies (such as the Willmore energy) have recently been obtained for certain special cases, such as triangulations of the sphere ([Xu, 2006](#)) and graphs of certain regular triangulations of the plane ([Xu et al., 2005](#); [Bobenko, 2008](#)). Our convergence result seems to be the first, though, to establish *uniform pointwise* convergence of 1-local discrete curvatures to principal curvatures of *arbitrary* immersed smooth surfaces.

Alternative approaches An alternative point of departure for establishing pointwise convergence of discrete curvatures is to give up k -local definitions of curvatures and to allow for $k \rightarrow \infty$ as the mesh refinement increases. In fact, the above mentioned convergence results of (ii) and (iii) may be interpreted in this way: by decreasing the diameter of the domains over which discrete curvatures are integrated (measured), while simultaneously increasing the mesh refinement inside these domains at a sufficiently fast rate, one recovers classical pointwise notions of smooth curvatures in the limit.

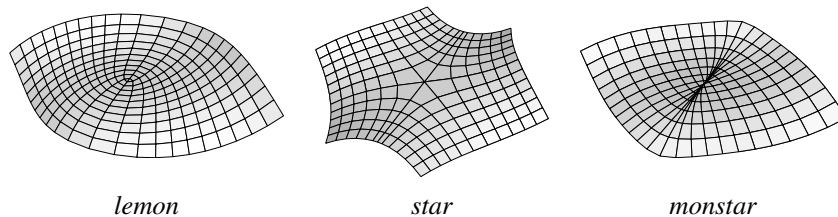


Figure 2: The three generic patterns of curvature lines near an umbilical point.

Similarly, as recently shown by [Belkin et al. \(2008\)](#), one obtains pointwise convergent kernel-based discrete Laplace operators by scaling the kernel used for approximating the smooth Laplacian, while simultaneously increasing the refinement of the kernel's support at a sufficiently fast rate. In contrast to these works, which need to allow for $k \rightarrow \infty$ to establish pointwise convergence, our result is obtained by working with the simplest and most local definition: $k = 1$.

2 Discrete curvatures from nets of curvature lines

In order to motivate our definition of discrete curvatures for nets of curvature lines, we recall some (more and less well-known) notions of curvature for planar polygonal curves and polyhedral surfaces. For a similar discussion, see [Sullivan \(2008\)](#).

2.1 Discrete curvatures of “Steiner-type”

Integrated curvatures for polygonal curves Generalizations of classical smooth notions of curvatures date back to [Steiner \(1840\)](#), who considered parallel offsets of convex hypersurfaces, relating *integrated* or *total* curvatures to changes in length, area, and enclosed volume. For a convex curve $\gamma \subset \mathbb{E}^2$, one of Steiner's formulas reads

$$l(\gamma_\epsilon) = l(\gamma) + \epsilon \int_\gamma \kappa(s) ds, \quad (1)$$

where l is the length functional and κ denotes the curve's curvature.

Steiner's formula can be extended to the non-smooth and non-convex case ([Federer, 1959](#); [Wintgen, 1982](#); [Zähle, 1986](#)), in particular providing notions of integrated curvatures for polygonal curves. Various notions of discrete curvatures for polygonal curves found in literature can be interpreted using offsets. Consider, e.g.,

$$\kappa_p \in \left\{ \theta_p, 2 \sin \frac{\theta_p}{2}, 2 \tan \frac{\theta_p}{2} \right\}, \quad (2)$$

where p denotes an inner vertex of a polygonal curve, and θ_p is the turning angle between the two line segments incident to p , whose sign is induced by the orientation of the curve. These notions are obtained by applying (1) to the three different types of

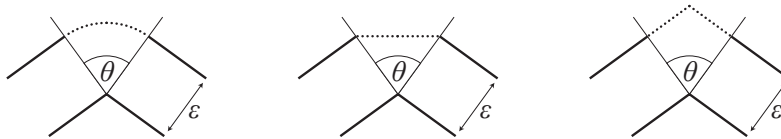


Figure 3: Applying Steiner’s formula (1) to the three depicted definitions of offset curves for a given polygonal curve lead to the three discrete curvatures in (2).

(parallel) offsets depicted in Figure 3. Among those, the first notion is the one considered by Steiner, the second corresponds to a finite element discretization using linear Lagrange elements, and the third arises naturally in the theory of discrete integrable systems (Bobenko and Suris, 1999; Hoffmann, 2008).

Integrated curvatures for polyhedral surfaces By a *polyhedral surface*, we mean a piecewise linear 2-manifold with finitely many vertices, straight edges, and flat faces. Extending the above notions of discrete curvatures from polygonal curves to oriented polyhedra leads to the following *edge-based* definitions of integrated normal curvatures:

$$\kappa_e \in \left\{ \theta_e \|\mathbf{e}\|, 2 \sin \frac{\theta_e}{2} \|\mathbf{e}\|, 2 \tan \frac{\theta_e}{2} \|\mathbf{e}\| \right\}. \quad (3)$$

Here $\theta_e \in (-\pi, \pi)$ is the angle between the normals of the two triangles incident to an edge \mathbf{e} , whose sign is induced by the orientation of the surface. Notice that κ_e measures curvature *orthogonal* to \mathbf{e} , since we assume that there is no curvature along \mathbf{e} itself. In the planar limit, $\theta_e \rightarrow 0$, the above definitions agree up to second order in the angle variable. Therefore, as it turns out, it will suffice to prove convergence of *one* of these definitions in order to obtain convergence for all of them. Convergence of the first definition in (3), in the sense of *measures*, was investigated in Fu (1993); Cohen-Steiner and Morvan (2006).

The above edge-based definitions give rise to *vertex-based* notions of integrated *mean curvatures*,

$$H_p = \frac{1}{2} \sum_{\mathbf{e} \sim p} \kappa_e, \quad (4)$$

by summing over the normal curvatures of all edges emanating from a given vertex p . The factor $1/2$ takes the meaning of distributing the normal curvature of each edge equally among its two adjacent vertices.

Finally, the scalar-valued definitions above can be extended to corresponding *vector-valued* notions. In the edge-based case, we obtain normal curvature vectors, \mathbf{k}_e , by multiplying κ_e with the (angle-bisecting) unit normal vector at edge \mathbf{e} (see Figure 4). Similarly, for each vertex p , we obtain mean curvature vectors, \mathbf{H}_p , as half the sum over the normal curvature vectors of the edges emanating from p . We remark that for $\kappa_e = 2 \sin \frac{\theta_e}{2} \|\mathbf{e}\|$, the resulting mean curvature vector coincides with the surface

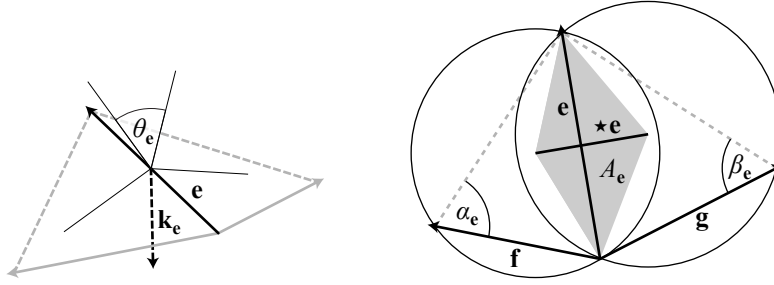


Figure 4: Edge-based quantities. *Left*: dihedral angle and discrete curvature vector. *Right*: dual edge and circumcentric area.

area gradient at p , when restricted to piecewise linear surface variations (the so-called *cotangent formula*, see [Pinkall and Polthier, 1993](#)). Its convergence in the sense of Sobolev norms was studied in [Hildebrandt et al. \(2006\)](#).

From integrated to pointwise curvatures In order to obtain *pointwise curvatures*, we divide the above integrated curvatures (associated with edges or vertices) by corresponding area measures. To obtain pointwise convergence, those areas have to be chosen carefully. We describe the construction of these area measures for *triangulated* polyhedral surfaces.

In the edge-based case, we consider what we call (signed) *circumcentric areas* (compare [Desbrun et al., 2005](#)). For each edge e we define

$$A_e = \frac{1}{2} \|e\| \|\star e\|, \quad (5)$$

where $\|\star e\|$ denotes (by abuse of notation) the *signed* length of the circumcentric dual edge, $\star e$. This dual edge intrinsically connects the circumcenters C_1 and C_2 of the two triangles T_1 and T_2 incident to e , where *intrinsic* means that one can think of T_1 and T_2 as being coplanar, see Figure 4. The sign of $\|\star e\|$ is positive if along the direction of the ray from C_1 through C_2 , triangle T_1 lies before T_2 , and negative otherwise. Notice that for a triangulated surface without boundary, the sum $\sum_e A_e$ is equal to the total surface area.

Similar to vertex-based integrated curvatures, we obtain vertex-based area measures from the edge-based case via

$$A_p = \frac{1}{2} \sum_{e \sim p} A_e, \quad (6)$$

where the sum is taken over all edges emanating from a given vertex p . Again, the factor $1/2$ takes the meaning of distributing each area measure equally among its two incident vertices.

Notice that A_p can be interpreted as the *Voronoi area* of p and is hence always positive. However, A_e may become zero or negative. Fortunately, for the special case

of nets of curvature lines, we are able to provide uniform positive lower (and upper) bounds for A_e (see Section 3.1).

2.2 Main result

A CW-complex is called *strongly regular* if all attaching maps are homeomorphisms and the intersection of any two cells is either empty or a single cell. We refer to a *discrete net* on a smooth surface, M , as the 1-skeleton of a strongly regular CW-complex with underlying space M . Throughout, we assume that the 1-cells of a discrete net are *smoothly* embedded into M . Note that a discrete net has the structure of a graph, $\Gamma = (V, E)$, with vertex set V and edge set E .

A *discrete net of curvature lines* is a special discrete net on an immersed surface $M \subset \mathbb{E}^3$, defined as follows. Each edge is part of an integral line along a principal curvature direction and each non-umbilical vertex has valence four. This definition encompasses spherical surface regions, where every direction is a principal direction.

Notation for vertices and edges Throughout, we consider discrete nets, $\Gamma = (V, E)$, on an isometrically immersed, oriented surface $M \subset \mathbb{E}^3$. For each (curved) edge, $e \in E$, we denote by \mathbf{e} its corresponding *straight* edge vector in \mathbb{E}^3 , obtained by connecting the endpoints of e . For each disjoint pair of edges $(e, f) \in E \times E$, incident to a common vertex p and contained in a common 2-cell, we consider the flat triangle spanned by \mathbf{e} and \mathbf{f} . For each vertex, $p \in V$, the union of these triangles forms the triangulated *vertex star*, $st(p)$. Under certain regularity conditions on the discrete net, we can apply the above (edge- and vertex-based) definitions of discrete (integrated and pointwise) curvatures to each vertex star. Out of the triangles in $st(p)$, we frequently consider two adjacent ones that are spanned by oriented edges \mathbf{e} , \mathbf{f} and \mathbf{g} , where \mathbf{e} denotes the common edge, see Figure 4. Denoting by \mathbf{n} the normal of M at p , we assume that $\mathbf{n} \cdot (\mathbf{e} \times \mathbf{f}) > 0$ and $\mathbf{n} \cdot (\mathbf{e} \times \mathbf{g}) < 0$.

Explicit constants We introduce those constants that appear throughout the text. Specifically, we avoid any hidden constants. For each $q \in M$, let $S(q)$ denote the shape (or Weingarten) operator. Our estimates depend on both S and its covariant derivative, ∇S . Accordingly, we define

$$\mathcal{K} := \sup_q \|S(q)\| \quad \text{and} \quad \mathcal{K}' := \sup_q \|(\nabla S)(q)\|, \quad (7)$$

where $\|\cdot\|$ denotes the usual tensor norm. We note that \mathcal{K} is an upper bound for the normal curvatures of M , whereas \mathcal{K}' provides an upper bound for the derivatives $\nabla_{\gamma'}(\kappa_{\gamma'})$ of the normal curvatures $\kappa_{\gamma'}$ along geodesics γ .

Let ϵ denote the *intrinsic* length of the longest edge, $e \in E$, that emanates from a given vertex p (denoted by $e \sim p$), i.e.,

$$\epsilon = \max_{e \sim p} l(e). \quad (8)$$

Here, l denotes the length functional for curves in \mathbb{E}^3 . Notice that each straight edge, \mathbf{e} , corresponding to $e \in E$, satisfies $\|\mathbf{e}\| \leq d_M(p, q) \leq \epsilon$, where $d_M(p, q)$ denotes the geodesic distance between the two endpoints of e .

Additionally, our estimates depend on *shape regularity*, or *aspect ratio*. Given $p \in V$, we define $\rho > 1$ such that for all straight edges emanating from p one has

$$\frac{\epsilon}{\rho} \leq \|\mathbf{e}\| \quad \text{as well as} \quad \frac{\|\mathbf{e}\| \|\mathbf{f}\|}{\|\mathbf{e} \times \mathbf{f}\|} \leq \rho, \quad (9)$$

where the latter relation is required to hold for all pairs (\mathbf{e}, \mathbf{f}) that form a triangle of $st(p)$. Notice that the former inequality implies $1/\rho \leq \|\mathbf{e}\|/\|\mathbf{f}\| \leq \rho$. Finally, we require the sampling condition

$$\epsilon \leq \frac{1}{16\mathcal{K}\rho^2}. \quad (10)$$

In some of our estimates, it will suffice to work with weaker sampling conditions, such as $\epsilon \leq \frac{1}{2\mathcal{K}\rho}$ or $\epsilon \leq \frac{1}{2\mathcal{K}}$, both of which are implied by (10).

Theorem 1. *Let $p \in V$ be vertex in a discrete net of curvature lines on a smooth, oriented, immersed surface, M , and assume the regularity and sampling conditions (9) and (10) in $st(p)$. If p is non-umbilical, then out of the four straight edges emanating from p , there are two edges \mathbf{e} and \mathbf{f} corresponding to the two principal directions \mathbf{v}_1 and \mathbf{v}_2 at p , respectively, such that*

$$\left| \kappa_1(p) - \frac{\kappa_{\mathbf{f}}}{2A_{\mathbf{f}}} \right| \leq C\epsilon \quad \text{and} \quad \left| \kappa_2(p) - \frac{\kappa_{\mathbf{e}}}{2A_{\mathbf{e}}} \right| \leq C\epsilon. \quad (11)$$

Here κ_i denotes the principal curvature corresponding to \mathbf{v}_i and $\kappa_{\mathbf{e}}, \kappa_{\mathbf{f}}$ and $A_{\mathbf{e}}, A_{\mathbf{f}}$ are as in (3) and (5), respectively. Similarly, if p is an arbitrary vertex (umbilical or not), then

$$\left| H(p) - \frac{H_p}{2A_p} \right| \leq C\epsilon, \quad (12)$$

where $H(p)$ is the mean curvature of M at p , while H_p and A_p are as in (4) and (6), respectively. In both estimates, the constant $C = C(\mathcal{K}, \mathcal{K}', \rho)$ is a function of \mathcal{K} , \mathcal{K}' and ρ only. Finally, by substituting ϵ and ρ by their respective maxima over all vertices $p \in V$, the above estimates provide a uniform error bound.

Remark. Equivalent estimates can be obtained when replacing the scalar-valued quantities in (11) and (12) by their corresponding vector-valued counterparts (for definitions, see Section 2). Proofs are nearly identical.

3 Proof of main result

The proof of Theorem 1 proceeds in several steps. First, we provide uniform lower and upper bounds for the circumcentric areas, $A_{\mathbf{e}}$ and A_p , as they appear in the denominator of (11) and (12) (see Section 3.1). In a second step, we provide estimates for

the edge-based curvature $\kappa_e = 2 \sin \frac{\theta_e}{2}$, by using its corresponding discrete curvature vector, \mathbf{k}_e . We establish that the projection of \mathbf{k}_e onto the tangent plane of M at p can be neglected. Furthermore, we show that the remaining normal component of \mathbf{k}_e leads to the estimates in Theorem 1 up to a certain error term (Section 3.2). While for general meshes the resulting error term cannot be controlled (and indeed causes failure of pointwise convergence), we provide uniform bounds for this error term for the specific case of nets of curvature lines (Section 3.3).

3.1 Uniform bounds for circumcentric areas

We provide uniform bounds for the edge-based and vertex-based circumcentric areas as defined by (5) and (6). These bounds hold on general discrete nets, not just on nets of curvature lines.

Edge-based case The circumcentric area of a straight edge, \mathbf{e} , can be expressed as

$$A_e = \frac{1}{4}(\cot \alpha_e + \cot \beta_e)\|\mathbf{e}\|^2 = \frac{\sin(\alpha_e + \beta_e)}{4 \sin \alpha_e \sin \beta_e} \|\mathbf{e}\|^2,$$

where α_e and β_e are the angles opposing \mathbf{e} in the two triangles meeting at \mathbf{e} , respectively (see Figure 4). Notice that if $\alpha_e \geq \delta$, $\beta_e \geq \delta$, and $\alpha_e + \beta_e \leq \pi - \delta$ for some $\delta > 0$, then

$$\sin \delta \|\mathbf{e}\|^2 \leq 4A_e \leq \frac{1}{\sin^2 \delta} \|\mathbf{e}\|^2, \quad (13)$$

which is precisely the kind of estimate we seek. Accordingly, we introduce the notion of δ -Delaunay edges, a nomenclature that is borrowed from the case of classical *Delaunay triangulations* (corresponding to $\delta = 0$).

Definition 1. An edge \mathbf{e} is called δ -Delaunay if there exists $\delta \geq 0$ such that $\alpha_e \geq \delta$, $\beta_e \geq \delta$, and $\alpha_e + \beta_e \leq \pi - \delta$.

As usual, we define discrete Gauss curvature at the vertex p as the angular defect, i.e., by $K_p = 2\pi - \sum_i \gamma_i$, where $\{\gamma_i\}$ are the intrinsic angles meeting at p . We obtain:

Lemma 1. Let p be of valence four, and let α_i, β_i denote the pairs of angles opposing the four edges emanating from p . Assume that $\alpha_i \geq \delta$ and $\beta_i \geq \delta$ for all $i = 1, \dots, 4$, as well as $K_p < 2\delta$. Then at least three out of the four edges meeting at p are δ -Delaunay.

Proof. Using that $K_p = -2\pi + \sum_{i=1}^4 (\alpha_i + \beta_i)$, the result follows from a straightforward calculation. \square

We show that the conditions of Lemma 1 are indeed satisfied using our assumptions on shape regularity (9) and on sampling density (10). To see this, first observe that (9) implies

$$\alpha_e \geq \sin \alpha_e = \frac{\|(\mathbf{f} - \mathbf{e}) \times \mathbf{f}\|}{\|(\mathbf{f} - \mathbf{e})\|\|\mathbf{f}\|} \geq \frac{\|\mathbf{e} \times \mathbf{f}\|}{(\rho + 1)\|\mathbf{e}\|\|\mathbf{f}\|} \geq \frac{1}{(\rho + 1)\rho} \geq \frac{1}{2\rho^2}, \quad (14)$$

where \mathbf{e} and \mathbf{f} are as before, and $\alpha_{\mathbf{e}}$ is the angle opposing \mathbf{e} in the triangle formed by \mathbf{e} and \mathbf{f} . Hence, the conditions of Lemma 1 on α_i and β_i are satisfied for $\delta = 1/(2\rho^2)$. It remains to check the condition on discrete Gauss curvature, K_p . We first note:

Lemma 2. *Assume that the normals of the triangles incident to p make an angle no greater than $\phi \in [0, \pi)$ with some fixed direction in \mathbb{E}^3 . Then $K_p \leq 2\pi(1 - \cos \phi)$.*

Proof. The unit normals to the triangles incident to p can be regarded as points on the unit 2-sphere. Then K_p is equal to the signed area of the region Ω on this sphere that is bounded by arcs of great circles connecting these unit normals. By assumption, Ω is contained in a geodesic disk of radius ϕ , the area of which is $2\pi(1 - \cos \phi)$. \square

In order to make use of the previous lemma, we seek a bound on the angle ϕ between the surface normal at $p \in M$ and the normals to the triangles incident to p . We infer from Morvan and Thibert (2004, Section 3, Corollary 1):

Lemma 3. *Let ϵ be as in (8), and assume the sampling condition $\epsilon \leq \frac{1}{2\mathcal{K}}$. Then the angle $\phi \in [0, \pi)$ between the surface normal at $p \in M$ and the normals to the triangles incident to p satisfies $\sin \phi \leq (4\rho + 2)\mathcal{K}\epsilon$, where \mathcal{K} and ρ are as in (7) and (9), respectively.*

Note that our assumptions are slightly different from those used in Morvan and Thibert (2004); in fact, our assumptions are stricter. While their sampling condition bounds the maximal extrinsic distance between two neighboring vertices, we consider the intrinsic length on the smooth surface, which is always larger. Additionally, Morvan and Thibert (2004) require that the distance between the discrete and the smooth surface is less than the *reach* of the smooth one. This requirement is implicitly fulfilled locally by our sampling condition $\epsilon \leq \frac{1}{2\mathcal{K}}$, since the reach is locally nothing but the minimal radius of curvature.

Lemma 4. *Let p be of valence four and assume the regularity and sampling conditions (9) and (10). Then at least three straight edges incident to p are δ -Delaunay for $\delta = \frac{1}{2\rho^2}$. Moreover, the circumcentric areas of these three edges are uniformly bounded from above and below by a function of ρ and ϵ .*

Proof. Using that $(1 - \cos \phi) \leq \sin^2 \phi$ for $\phi \in [-\frac{\pi}{2}, \frac{\pi}{2}]$, Lemmas 2 and 3 show that the discrete Gauss curvature at p satisfies

$$K_p \leq 2\pi(4\rho + 2)^2 \mathcal{K}^2 \epsilon^2 \leq (16\mathcal{K}\rho\epsilon)^2 .$$

Setting $\delta = \frac{1}{2\rho^2}$, the sampling condition (10) implies $K_p \leq 2\delta$. Moreover, (14) implies $\alpha_i \geq \delta$ and $\beta_i \geq \delta$ for all pairs of angles α_i, β_i opposing the four straight edges emanating from p . Finally, Lemma 1 and (13) imply the claim. \square

Applying the previous lemma to nets of curvature lines gives:

Proposition 1. *Let p be a vertex of valence four in a discrete net on M , and assume the regularity and sampling conditions (9) and (10). Then for at least three of the straight edges emanating from p , one has*

$$\frac{1}{C}\epsilon^2 \leq A_{\mathbf{e}} \leq C\epsilon^2 ,$$

where the constant C depends only on ρ .

Vertex-based case Thus far, we have treated the case of edge-base circumcentric areas, as required for approximating principal curvatures in Theorem 1. We now turn to the case of mean curvature, where we seek a bound on vertex-based areas, A_p . Similarly to Proposition 1 we obtain:

Proposition 2. *Let p be a vertex of a discrete net on M , and assume the regularity and sampling conditions (9) and (10). Then*

$$\frac{1}{C}\epsilon^2 \leq A_p \leq C\epsilon^2 ,$$

where the constants C only depends on ρ .

Proof. By (6), each A_p equals the Voronoi area of p , with respect to its 1-ring, on the cone spanned by the triangles containing p . Therefore, A_p is bounded from below by the squared length of the shortest edge emanating from p , multiplied by $(\pi - K_p/2)$. By (9), the length of the shortest edge is bounded from below by ϵ/ρ . Moreover, using the same arguments as in the proof of Lemma 4, we obtain $K_p \leq 1/\rho^2 \leq 1$. This gives the lower bound for A_p . Finally, by the definition of A_p , the upper bound follows from the upper bounds on each A_e , which were shown above. \square

3.2 The discrete curvature vector in Monge coordinates

In order to compare discrete to smooth curvatures, it will be beneficial to work with the discrete curvature *vector* (see Section 2.1), instead of working with the scalar discrete curvatures directly. Specifically, we work with the curvature vector, \mathbf{k}_e , corresponding to the scalar curvature $\kappa_e = 2 \sin \frac{\theta_e}{2} \|\mathbf{e}\|$. Using the notation introduced in Section 2.2, a straightforward calculation shows

$$\mathbf{k}_e = J_{\mathbf{f}}\mathbf{e} + J_{\mathbf{g}}\mathbf{e} , \tag{15}$$

where $J_{\mathbf{f}}$ and $J_{\mathbf{g}}$ denote rotations by $\frac{\pi}{2}$ around the axes $\mathbf{e} \times \mathbf{f}$ and $\mathbf{e} \times \mathbf{g}$, respectively (see Figure 5). Additionally, one finds that

$$J_{\mathbf{f}}\mathbf{e} = \frac{\mathbf{e}^2\mathbf{f} - (\mathbf{f} \cdot \mathbf{e})\mathbf{e}}{\|\mathbf{e} \times \mathbf{f}\|} , \tag{16}$$

and analogously for $J_{\mathbf{g}}\mathbf{e}$, where henceforth we will write $\mathbf{e}^2 = \mathbf{e} \cdot \mathbf{e}$.

Darboux frame and Monge coordinates The Darboux frame at $p \in M$ is given by $(\mathbf{v}_1, \mathbf{v}_2, \mathbf{n})$, where \mathbf{v}_1 and \mathbf{v}_2 are the (normalized) principal directions of M , and $\mathbf{n} = \mathbf{v}_1 \times \mathbf{v}_2$ is the surface normal. The coordinates corresponding to this frame are called *Monge coordinates*. We denote the components of a vector \mathbf{e} represented in these coordinates by (e_1, e_2, e_n) . In order to estimate the normal component of our discrete curvature vector, we start with a general result:

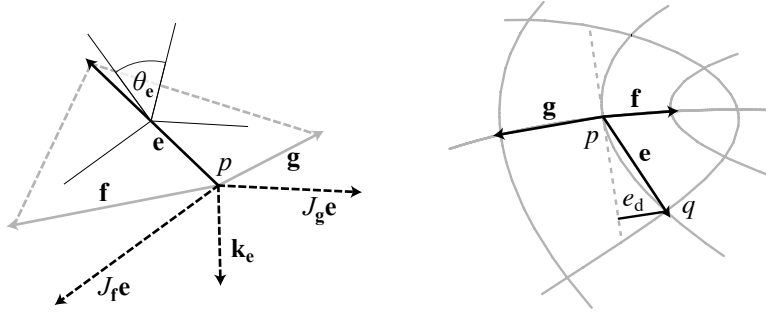


Figure 5: Edge-based quantities. *Left*: discrete curvature vector. *Right*: tangential deviation of a straight edge e .

Lemma 5. *In a discrete net on M , consider a vertex $p \in V$ and an incident edge $e \in E$ with corresponding straight edge vector, $\mathbf{e} = (e_1, e_2, e_n)$, in Monge coordinates around p . Let ϵ be as in (8) and assume the sampling condition $\epsilon \leq \frac{1}{2\mathcal{K}}$, where \mathcal{K} is given by (7). Then the normal component of \mathbf{e} satisfies*

$$|e_n| \leq \mathcal{K} \mathbf{e}^2 \leq \mathcal{K} \epsilon^2.$$

Furthermore, let $P(x, y) = \frac{\kappa_1}{2} x^2 + \frac{\kappa_2}{2} y^2$ denote the osculating paraboloid. Then

$$|e_n - P(e_1, e_2)| \leq \frac{\mathcal{K}' + 7\mathcal{K}^2}{3} \epsilon^3,$$

with \mathcal{K}' given by (7).

Proof. See appendix. □

We introduce the function

$$\delta_\kappa(p) = \kappa_2(p) - \kappa_1(p)$$

which will play an important role later. We drop the argument p wherever this causes no confusion.

Lemma 6. *With the same assumptions as in Lemma 5, we have*

$$\begin{aligned} e_n &= \frac{\kappa_1}{2} \mathbf{e}^2 + \frac{\delta_\kappa}{2} e_2^2 + \mathcal{O}(\epsilon^3) \\ &= \frac{\kappa_2}{2} \mathbf{e}^2 - \frac{\delta_\kappa}{2} e_1^2 + \mathcal{O}(\epsilon^3), \end{aligned}$$

where the constant in $\mathcal{O}(\epsilon^3)$ depends only on \mathcal{K} and \mathcal{K}' .

Proof. From Lemma 5, we deduce that

$$\begin{aligned} e_n &= \frac{\kappa_1}{2} e_1^2 + \frac{\kappa_2}{2} e_2^2 + \mathcal{O}(\epsilon^3) \\ &= \frac{\kappa_1}{2} (e_1^2 + e_2^2) + \frac{\delta_\kappa}{2} e_2^2 + \mathcal{O}(\epsilon^3) \\ &= \frac{\kappa_1}{2} \mathbf{e}^2 + \frac{\delta_\kappa}{2} e_2^2 + \mathcal{O}(\epsilon^3). \end{aligned}$$

The last line follows from Lemma 5 and the condition $\epsilon \leq \frac{1}{2\mathcal{K}}$, which together ensure that $e_n^2 \leq \frac{\mathcal{K}}{2} \epsilon^3$. The second equation in the statement of the lemma follows analogously. \square

We consider the splitting $\mathbf{k}_e = (\mathbf{k}_e)_t + (\mathbf{k}_e)_n$ of the discrete curvature vector (15) into tangential and normal components with respect to the Darboux frame. We show that the normal component of \mathbf{k}_e leads to the desired approximation of the principal curvatures of the smooth surface, while its tangential component is negligible.

Lemma 7. *Under the same assumptions as in Lemma 5, the projection of the discrete curvature vector onto the tangent plane at $p \in M$ satisfies $\|(\mathbf{k}_e)_t\| \leq 10\mathcal{K}^2 \rho^2 \epsilon^3$.*

Proof. See appendix. \square

In what follows, we require the notion of *tangential deviation* of a straight edge.

Definition 2. *Consider a straight edge, \mathbf{e} , emanating from a point p in a discrete net on M . If \mathbf{e} is associated with the principal direction \mathbf{v}_1 , then its tangential deviation, e_d , from its associated principal direction, measures its component along \mathbf{v}_2 , i.e., $e_d = |e_2|$ (see Figure 5). Similarly, if \mathbf{e} is associated with \mathbf{v}_2 , then $e_d = |e_1|$.*

The following result expresses the error between discrete and smooth principal curvatures in terms of tangential deviations.

Proposition 3. *In a discrete net on M , associate \mathbf{e} with the principal direction \mathbf{v}_1 , and associate \mathbf{f} and \mathbf{g} with \mathbf{v}_2 , as in Figure 5. Let A_e be as in (13). Then, under the assumptions of Lemma 5, we have*

$$|\kappa_e - 2A_e \kappa_2| \leq C (|\delta_\kappa (e_d + f_d + g_d)| \epsilon + \epsilon^3),$$

where $C = C(\mathcal{K}, \mathcal{K}', \rho)$ and $(\cdot)_d$ denotes the respective tangential deviations.

Proof. In order to estimate the normal component, $(\mathbf{k}_e)_n = (\mathbf{J}_f \mathbf{e})_n + (\mathbf{J}_g \mathbf{e})_n$, of the discrete curvature vector, we use (16) to obtain

$$(\mathbf{J}_f \mathbf{e})_n = \frac{\mathbf{e}^2 f_n - (\mathbf{f} \cdot \mathbf{e}) e_n}{\|\mathbf{e} \times \mathbf{f}\|},$$

and analogously for $(\mathbf{J}_g \mathbf{e})_n$. Similarly, the circumcentric area can be written as a sum $A_e = A_{e,f} + A_{e,g}$, where

$$A_{e,f} = \frac{\mathbf{f} \cdot (\mathbf{f} - \mathbf{e})}{4\|\mathbf{e} \times \mathbf{f}\|} \mathbf{e}^2,$$

and analogously for $A_{\mathbf{e},\mathbf{g}}$. Using this expression and applying Lemma 6 to the above expression for $(\mathbf{J}_{\mathbf{f}}\mathbf{e})_n$, we obtain

$$\begin{aligned} (\mathbf{J}_{\mathbf{f}}\mathbf{e})_n &= \frac{\mathbf{e}^2(\kappa_2\mathbf{f}^2 + \delta_\kappa f_1^2) - \mathbf{f} \cdot \mathbf{e}(\kappa_2\mathbf{e}^2 + \delta_\kappa e_1^2)}{2\|\mathbf{e} \times \mathbf{f}\|} + \mathcal{O}(\epsilon^3) \\ &= 2A_{\mathbf{e},\mathbf{f}}\kappa_2 + \delta_\kappa f_1^2 \frac{\mathbf{e}^2}{2\|\mathbf{e} \times \mathbf{f}\|} + \delta_\kappa \mathbf{f} \cdot \mathbf{e} \frac{e_1^2}{2\|\mathbf{e} \times \mathbf{f}\|} + \mathcal{O}(\epsilon^3), \end{aligned}$$

and analogously for $(\mathbf{J}_{\mathbf{g}}\mathbf{e})_n$. Applying the shape regularity condition (9) yields

$$|(\mathbf{J}_{\mathbf{f}}\mathbf{e})_n - 2A_{\mathbf{e},\mathbf{f}}\kappa_2| \leq C(|\delta_\kappa(f_1^2 + \mathbf{f} \cdot \mathbf{e})| + \epsilon^3).$$

Using $|\mathbf{f} \cdot \mathbf{e}| \leq |e_2 + f_1|\epsilon + \mathcal{O}(\epsilon^4)$, we arrive at

$$|(\mathbf{k}_{\mathbf{e}})_n - 2A_{\mathbf{e}}\kappa_2| \leq C(|\delta_\kappa(e_d + f_d + g_d)|\epsilon + \epsilon^3),$$

implying the claim, since the tangential part, $(\mathbf{k}_{\mathbf{e}})_t$, is of order $\mathcal{O}(\epsilon^3)$ by Lemma 7. \square

From the preceding proposition, we deduce that in order to obtain the desired estimate $|\kappa_{\mathbf{e}} - 2A_{\mathbf{e}}\kappa_2| \leq C\epsilon^3$, it is sufficient to show that

$$|\delta_\kappa(p)e_d| \leq C\epsilon^2 \tag{17}$$

for all edges \mathbf{e} emanating from p . There is a simple case, where (17) is obviously fulfilled: let M be a paraboloid, and let p be its apex. Consider four edges along the principal directions, emanating from p . Then for any edge \mathbf{e} out of these four, its tangential deviation, e_d , from its associated principal direction is zero, so the left hand side of (17) vanishes.

3.3 Specific estimates for nets of curvature lines

The essential difference between nets of curvature lines on arbitrary smooth surfaces and the above paraboloid example is the fact that curvature lines usually have geodesic curvature, κ^g . While the tangential deviation, e_d , can be bounded by $C\epsilon^2$, with C depending on \mathcal{K} and κ^g , this does not suffice for a uniform error bound, since κ^g may blow up at umbilical points. Perhaps surprisingly, though, the product, $|\delta_\kappa(p)e_d|$, can be bounded for nets of curvature lines, as the following result shows. Notably, this result is *specific* to nets of curvature lines, and does not hold for arbitrary nets.

Lemma 8. *Let \mathbf{e} be an edge emanating from p in a discrete net of curvature lines. Then*

$$|\delta_\kappa(p)e_d| \leq (\mathcal{K}^2 + 4\mathcal{K}')\epsilon^2,$$

where e_d is the tangential deviation of \mathbf{e} from its associated principal curvature direction, as above.

The intuition behind this statement is as follows. Roughly, e_d is proportional to the geodesic curvature of the curvature line corresponding to \mathbf{e} . This geodesic curvature, in turn, is inverse proportional to δ_κ , as the next lemma shows. Therefore, the product $\delta_\kappa e_d$ can be uniformly bounded.

Lemma 9. *The geodesic curvature of the principal curvature line along \mathbf{v}_1 satisfies*

$$\kappa_{\mathbf{v}_1}^g = \frac{\nabla_{\mathbf{v}_2} \kappa_1}{\kappa_1 - \kappa_2} \quad \text{and} \quad |\kappa_{\mathbf{v}_1}^g| \leq \frac{\mathcal{K}'}{|\kappa_1 - \kappa_2|},$$

where κ_1 and κ_2 denote the principal curvatures corresponding to the principal directions \mathbf{v}_1 and \mathbf{v}_2 , respectively.

Proof. Since \mathbf{v}_1 and \mathbf{v}_2 are the orthogonal eigenvectors of the shape operator S , one has $S\mathbf{v}_1 \cdot \mathbf{v}_2 = 0$. We use the Frenet formulas, $\nabla_{\mathbf{v}_1} \mathbf{v}_1 = \kappa_{\mathbf{v}_1} \mathbf{v}_2$ and $\nabla_{\mathbf{v}_1} \mathbf{v}_2 = -\kappa_{\mathbf{v}_1} \mathbf{v}_1$, as well as the Codazzi-Mainardi equation, $(\nabla_{\mathbf{u}} S)\mathbf{v} = (\nabla_{\mathbf{v}} S)\mathbf{u}$, to obtain

$$\begin{aligned} 0 &= \nabla_{\mathbf{v}_1} (S\mathbf{v}_1 \cdot \mathbf{v}_2) \\ &= (\nabla_{\mathbf{v}_1} S)\mathbf{v}_1 \cdot \mathbf{v}_2 + S(\nabla_{\mathbf{v}_1} \mathbf{v}_1) \cdot \mathbf{v}_2 + S\mathbf{v}_1 \cdot \nabla_{\mathbf{v}_1} \mathbf{v}_2 \\ &= \nabla_{\mathbf{v}_2} (S\mathbf{v}_1 \cdot \mathbf{v}_1) - S(\nabla_{\mathbf{v}_2} \mathbf{v}_1) \cdot \mathbf{v}_1 - S\mathbf{v}_1 \cdot \nabla_{\mathbf{v}_2} \mathbf{v}_1 + \kappa_{\mathbf{v}_1}^g (\kappa_2 - \kappa_1) \\ &= \nabla_{\mathbf{v}_2} \kappa_1 + \kappa_{\mathbf{v}_1}^g (\kappa_2 - \kappa_1), \end{aligned}$$

proving the first part. The second part follows from the definition of \mathcal{K}' . \square

Proof of Lemma 8. Let $\gamma : [0, \epsilon] \rightarrow M$ be the curvature line associated with \mathbf{e} , parameterized by arc-length, passing through $p = \gamma(0)$. By definition, e_d is bounded by the maximal distance from γ to the tangent line passing through $\gamma'(0)$. Since γ is parameterized by arc-length, we obtain

$$e_d \leq \frac{\mathcal{K}_\gamma}{2} \epsilon^2,$$

where \mathcal{K}_γ denotes the maximal curvature of γ as a space curve. Decomposing the curvature of γ into its normal and geodesic curvature components, with respect to M , and using Lemma 9, yields

$$\mathcal{K}_\gamma \leq \mathcal{K}_\gamma^n + \mathcal{K}_\gamma^g \leq \mathcal{K} + \sup_{s \in [0, \epsilon]} \frac{\mathcal{K}'}{|\delta_\kappa(\gamma(s))|}, \quad (18)$$

where \mathcal{K}_γ^n and \mathcal{K}_γ^g denote the maximal normal and geodesic curvature, respectively. Consequently, we now seek a lower bound for $\delta_\kappa(\gamma(s))$. To do so, first observe that by (7) and the Frenet formulas (see above), the derivatives of κ_1 and κ_2 are bounded by \mathcal{K}' . Hence, the function δ_κ is Lipschitz with constant $L = 2\mathcal{K}'$, i.e.,

$$|\delta_\kappa(p) - \delta_\kappa(q)| \leq L d_M(p, q),$$

for every point $q \in M$. We now distinguish two cases: (i) $|\delta_\kappa(p)| < 2L\epsilon$ and (ii) $|\delta_\kappa(p)| \geq 2L\epsilon$. In the first case, we immediately obtain

$$|\delta_\kappa(p)e_d| \leq 2L\epsilon^2 = 4\mathcal{K}'\epsilon^2,$$

which already proves the claim of the lemma. In the second case, observe that

$$|\delta_\kappa(\gamma(s))| \geq |\delta_\kappa(p)| - L\epsilon \geq \frac{1}{2}|\delta_\kappa(p)|.$$

Plugging this into (18) gives

$$\mathcal{K}_\gamma \leq \mathcal{K} + \frac{2\mathcal{K}'}{|\delta_\kappa(p)|}.$$

Together this yields

$$|\delta_\kappa(p)e_d| \leq |\delta_\kappa(p)| \left(\frac{\mathcal{K}}{2} + \frac{\mathcal{K}'}{|\delta_\kappa(p)|} \right) \epsilon^2 \leq (\mathcal{K}^2 + \mathcal{K}')\epsilon^2,$$

completing the proof. \square

3.4 Putting things together

Associating \mathbf{e} with the principal curvature direction \mathbf{v}_1 , and \mathbf{f} and \mathbf{g} with \mathbf{v}_2 , we obtain from Proposition 3 and Lemma 8 that there exists a constant $C = C(\mathcal{K}, \mathcal{K}', \rho)$ such that

$$|\kappa_{\mathbf{e}} - 2A_{\mathbf{e}}\kappa_2| \leq C\epsilon^3. \quad (19)$$

Proposition 1 shows that $A_{\mathbf{e}}$ is bounded from below and above by $(1/C)\epsilon^2$ and $C\epsilon^2$, respectively, with $C = C(\rho)$. Therefore, we can divide (19) by $A_{\mathbf{e}}$ to obtain the first part of Theorem 1. The proof of the second part is similar, and it will only be sketched here. If p is not umbilical, let A_i be the sum of the two circumcentric areas corresponding to the edges associated with \mathbf{v}_i . Applying (19) yields

$$\begin{aligned} H_p &= \frac{1}{2}(2A_2\kappa_1 + 2A_1\kappa_2) + \mathcal{O}(\epsilon^3) \\ &= 2A_p H(p) + \frac{\delta_\kappa}{2}(A_1 - A_2) + \mathcal{O}(\epsilon^3). \end{aligned}$$

The expression $\delta_\kappa(A_1 - A_2)$ can now be bounded using similar arguments as in the proof of Proposition 3, giving

$$H_p = 2A_p H(p) + \mathcal{O}(\epsilon^3), \quad (20)$$

with $C = C(\mathcal{K}, \mathcal{K}', \rho)$. The same formula holds if p is an umbilical vertex. To see this, simply apply (19) to definitions (4) and (6) and observe that $H(p) = \kappa_1(p) = \kappa_2(p)$. Finally, the area bound from Proposition 2 allows for dividing (20) by A_p , giving the second part of Theorem 1.

4 Numerical experiments

We present numerical tests to illustrate our convergence result. Using numerical integration with the Mathematica method `NDSolve`, we integrated the principal curvature directions \mathbf{v}_1 and \mathbf{v}_2 in the parameter domain, i.e., by solving the ODEs

$$\gamma_1'(s) = \mathbf{v}_1(\gamma_1(s)) \quad \text{and} \quad \gamma_2'(s) = \mathbf{v}_2(\gamma_2(s)).$$

We then computed the intersection points of the curvature lines, γ_1 and γ_2 , to obtain a discrete net. Figure 2 shows the result for the graphs of three different functions of the form

$$h(x, y) = \frac{1}{2}\kappa(x^2 + y^2) + \frac{1}{6}(px^3 + 3qx^2y + 3rxy^2 + sy^3),$$

where we used $(p = 1.8, r = 0.6)$, $(p = 0, r = 0.8)$, $(p = 1.8, r = 1.2)$, and $\kappa = q = s = 0$, corresponding to the three generic patterns of curvature lines (see Darboux (1896); Berry and Hannay (1977)).

Finally, we refined the net successively. For each level, we computed the *maximal* error between our discrete pointwise curvature estimations and the exact values of the corresponding principal curvatures. Results are shown in Figure 6, numerically confirming *linear convergence* in mesh size. Observe that in the third case (corresponding to the so-called monstar-type umbilic), the aspect ratio of the triangles incident to the umbilical point blows up. Despite this effect, we still observe numerical convergence of our discrete curvatures, suggesting that even a weaker assumption on shape regularity than ours might be sufficient for convergence. The extremely short edges appearing in our refinement sequence for the monstar-type umbilic are the reason why our numerical experiments in this case could only be performed up to $n = 256$.

5 Conclusion

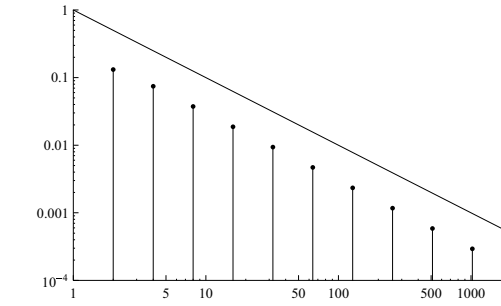
While pointwise convergence of discrete curvatures cannot be expected for general meshes, our results show that nets of curvature lines provide the necessary additional structure required for uniform *pointwise* convergence. An important aspect of our analysis is that our estimates hold up to, and including, umbilical points.

We view our result as a first step for studying a purely discrete framework. Indeed, discrete counterparts of nets of curvature lines are provided by so-called *circular* or *conical* nets (Bobenko, 2008; Liu et al., 2006). We hope that our work provides a starting point for investigating convergence of discrete curvatures on these purely discrete differential geometric objects.

References

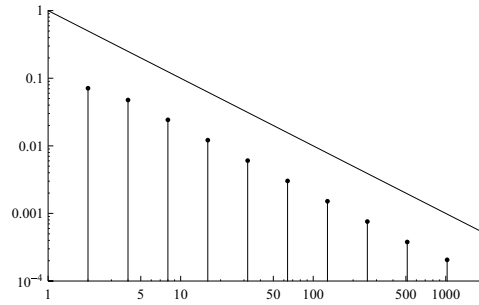
- M. Belkin, J. Sun, and Y. Wang. [Discrete laplace operator on meshed surfaces](#). In *Proceedings SCG '08*, pages 278–287, 2008.
- M. V. Berry and J. H. Hannay. [Umbilic points on gaussian random surfaces](#). *J. Phys. A: Math. Gen.*, 10:1809–1821, 1977.
- A. Bobenko, P. Schröder, J. Sullivan, and G. Ziegler, editors. *Discrete Differential Geometry*, volume 38 of *Oberwolfach Seminars*, 2008. Birkhäuser.
- A. I. Bobenko. [Surfaces from Circles](#). In *Discrete Differential Geometry*, volume 38 of *Oberwolfach Seminars*, pages 3–36. Birkhäuser, 2008.

n	max. error lemon
2	$1.32 \cdot 10^{-1}$
4	$7.44 \cdot 10^{-2}$
8	$3.75 \cdot 10^{-2}$
16	$1.87 \cdot 10^{-2}$
32	$9.37 \cdot 10^{-3}$
64	$4.69 \cdot 10^{-3}$
128	$2.34 \cdot 10^{-3}$
256	$1.17 \cdot 10^{-3}$
512	$5.85 \cdot 10^{-4}$
1024	$2.93 \cdot 10^{-4}$



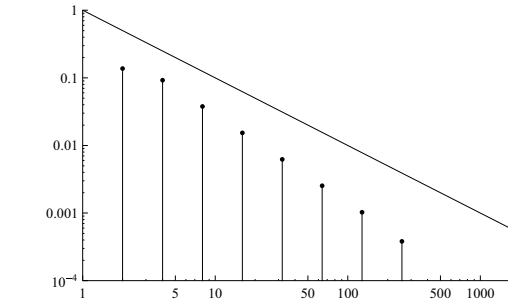
lemon ($p = 1.8, r = 0.6$)

n	max. error star
2	$7.10 \cdot 10^{-2}$
4	$4.76 \cdot 10^{-2}$
8	$2.42 \cdot 10^{-2}$
16	$1.22 \cdot 10^{-2}$
32	$6.06 \cdot 10^{-3}$
64	$3.03 \cdot 10^{-3}$
128	$1.51 \cdot 10^{-3}$
256	$7.57 \cdot 10^{-4}$
512	$3.79 \cdot 10^{-4}$
1024	$2.06 \cdot 10^{-4}$



star ($p = 0, r = 0.8$)

n	max. error monstar
2	$1.37 \cdot 10^{-1}$
4	$9.22 \cdot 10^{-2}$
8	$3.78 \cdot 10^{-2}$
16	$1.53 \cdot 10^{-2}$
32	$6.23 \cdot 10^{-3}$
64	$2.53 \cdot 10^{-3}$
128	$1.02 \cdot 10^{-3}$
256	$3.81 \cdot 10^{-4}$



monstar ($p = 1.8, r = 1.2$)

Figure 6: Approximation error under refinement of discrete nets of curvature lines. In a doubly logarithmic plot, the x -axis shows the number of subdivisions of the unit interval; the y -axis shows maximal pointwise error. The solid line shows the function $\frac{1}{x}$ to indicate the slope corresponding to linear convergence.

- A. I. Bobenko and Y. Suris. [Discrete Time Lagrangian Mechanics on Lie Groups, with an Application to the Lagrange Top](#). *Comm. Math. Phys.*, 204(1):147–188, 1999.
- F. Cazals and M. Pouget. [Estimating differential quantities using polynomial fitting of osculating jets](#). *Comput. Aided Geom. Des.*, 22(2):121–146, 2005.
- D. Cohen-Steiner and J.-M. Morvan. [Second fundamental measure of geometric sets and local approximation of curvatures](#). *J. Differential Geom.*, 73(3):363–394, 2006.
- G. Darboux. *Leçons Sur La Theorie Generale Des Surfaces*, volume 4, chapter VII, pages 448–465. Gauthier-Villars et fils, Paris, 1896.
- M. Desbrun, A. N. Hirani, M. Leok, and J. E. Marsden. [Discrete exterior calculus](#). Arxiv preprint, 2005.
- G. Dziuk. [Finite Elements for the Beltrami operator on arbitrary surfaces](#). In *Partial differential equations and calculus of variations*, volume 1357 of *Lecture Notes in Mathematics*, pages 142–155. Springer, 1988.
- H. Federer. [Curvature measures](#). *Trans. Amer. Math.*, 93(3):418–491, 1959.
- J. H. G. Fu. [Convergence of curvatures in secant approximations](#). *J. Differential Geom.*, 37:177–190, 1993.
- E. Grinspun and M. Desbrun, editors. [Discrete differential geometry: an applied introduction](#), ACM SIGGRAPH Courses Notes, 2006. ACM Press New York, NY, USA.
- K. Hildebrandt, K. Polthier, and M. Wardetzky. [On the convergence of metric and geometric properties of polyhedral surfaces](#). *Geom. Dedicata*, 123(1):89–112, 2006.
- T. Hoffmann. [Discrete Hashimoto Surfaces and a Doubly Discrete Smoke-Ring Flow](#). In *Discrete Differential Geometry*, volume 38 of *Oberwolfach Seminars*, pages 95–116. Birkhäuser, 2008.
- Y. Liu, H. Pottmann, J. Wallner, Y.-L. Yang, and W. Wang. [Geometric modeling with conical meshes and developable surfaces](#). *ACM Trans. Graph.*, 25(3):681–689, 2006.
- D. S. Meek and D. J. Walton. [On surface normal and Gaussian curvature approximations given data sampled from a smooth surface](#). *Comput. Aided Geom. Des.*, 17(6):521–543, 2000.
- J.-M. Morvan and B. Thibert. [Approximation of the normal vector field and the area of a smooth surface](#). *Discr. Comp. Geom.*, 32(3):383–400, 2004.
- U. Pinkall and K. Polthier. [Computing discrete minimal surfaces and their conjugates](#). *Exp. Math.*, 2(1):15–36, 1993.
- J. Steiner. Ueber parallele Flächen. *Monatsbericht der Akademie der Wissenschaften zu Berlin*, pages 114–118, 1840.
- J. M. Sullivan. [Curves of Finite Total Curvature](#). In *Discrete Differential Geometry*, volume 38 of *Oberwolfach Seminars*, pages 137–162. Birkhäuser, 2008.

- P. Wintgen. Normal cycle and integral curvature for polyhedra in Riemannian manifolds. In Soós and Szenthe, editors, *Differential Geometry*, pages 805–816. 1982.
- G. Xu. [Discrete Laplace-Beltrami Operator on Sphere and Optimal Spherical Triangulations](#). *Int. J. Comp. Geom. Appl.*, 16(1):75–93, 2006.
- Z. Xu, G. Xu, and J.-G. Sun. [Convergence analysis of discrete differential geometry operators over surfaces](#). In *Mathematics of Surfaces XI*, volume 3604 of *LNCS*, pages 448–457. Springer, 2005.
- M. Zähle. [Integral and current representations of Federer’s curvature measures](#). *Arch. Math.*, 46:557–567, 1986.

Appendix

Proof of Lemma 5. In Monge coordinates at the point p , M is parameterized as a graph of a height function $h(x, y)$. From now on, let $\mathbf{e} = (x, y, h(x, y))$.

Let $\mathbf{v} = \frac{(x, y)}{\|(x, y)\|}$ and $d = \|(x, y)\|$, and note that $d = \|\mathbf{e}_t\| \leq \|\mathbf{e}\|$. Let $D_{\mathbf{v}}^i h$ denote the i th directional derivative of h in direction \mathbf{v} and $D^i h$ denote the i th total derivative. We have

$$\begin{aligned} h(x, y) &= \int_0^d \int_0^t D_{\mathbf{v}}^2 h(t) d\tau dt \\ &= \int_0^d \int_0^t \left(D_{\mathbf{v}}^2 h(0) + \int_0^\tau D_{\mathbf{v}}^3 h(\sigma \mathbf{v}) d\sigma \right) d\tau dt, \end{aligned} \quad (21)$$

so the difference between the normal component of surface to its osculating paraboloid, $P(x, y)$, is exactly the triple integral over the third derivatives

$$|h(x, y) - P(x, y)| = \left| \int_0^d \int_0^t \int_0^\tau D_{\mathbf{v}}^3 h(\sigma \mathbf{v}) d\sigma d\tau dt \right|. \quad (22)$$

We now bound the second and third derivatives of h in terms of \mathcal{K} and \mathcal{K}' . Let $I(\cdot, \cdot)$ and $II(\cdot, \cdot) = I(S\cdot, \cdot)$ denote the first and second fundamental form, respectively. We use

$$I(\mathbf{u}, \mathbf{v}) = \mathbf{u}^T (\text{Id} + Dh Dh^T) \mathbf{v} \quad (23)$$

as well as

$$\kappa_{\mathbf{v}} = \frac{II(\mathbf{v}, \mathbf{v})}{I(\mathbf{v}, \mathbf{v})} = \frac{I(S\mathbf{v}, \mathbf{v})}{I(\mathbf{v}, \mathbf{v})} = \frac{D_{\mathbf{v}}^2 h}{\sqrt{1 + \|Dh\|^2} I(\mathbf{v}, \mathbf{v})}, \quad (24)$$

to obtain the estimate

$$|D_{\mathbf{v}}^2 h| = |\kappa_{\mathbf{v}}| \sqrt{1 + \|Dh\|^2} I(\mathbf{v}, \mathbf{v}) \leq |\kappa_{\mathbf{v}}| (1 + \|Dh\|^2)^{\frac{3}{2}}. \quad (25)$$

Taking another derivative in direction \mathbf{v} yields

$$\begin{aligned} D_{\mathbf{v}}^3 h &= D_{\mathbf{v}}(\kappa_{\mathbf{v}}) \sqrt{1 + \|Dh\|^2} I(\mathbf{v}, \mathbf{v}) \\ &\quad + \kappa_{\mathbf{v}} D_{\mathbf{v}} \left(\sqrt{1 + \|Dh\|^2} \right) I(\mathbf{v}, \mathbf{v}) \\ &\quad + \kappa_{\mathbf{v}} \sqrt{1 + \|Dh\|^2} D_{\mathbf{v}}(I(\mathbf{v}, \mathbf{v})). \end{aligned} \quad (26)$$

To bound the first term, we use (24) and $\nabla I \equiv 0$ to derive

$$D_{\mathbf{v}} \kappa_{\mathbf{v}} = \frac{I((\nabla_{\mathbf{v}} S)\mathbf{v}, \mathbf{v}) + 2I(S\mathbf{v}, \nabla_{\mathbf{v}} \mathbf{v}) - 2\kappa_{\mathbf{v}} I(\mathbf{v}, \nabla_{\mathbf{v}} \mathbf{v})}{I(\mathbf{v}, \mathbf{v})}. \quad (27)$$

Using the Koszul formula for the Levi-Civita connection and applying (23), we obtain

$$I(\nabla_{\mathbf{v}} \mathbf{v}, \mathbf{w}) = 2\mathbf{v}^T (D^2 h)_{\mathbf{v}} Dh^T \mathbf{w} - \mathbf{v}^T (D^2 h)_{\mathbf{w}} Dh^T \mathbf{v}.$$

Together with (24), this leads to the estimate

$$|I(\nabla_{\mathbf{v}}\mathbf{v}, \mathbf{w})| \leq 3\mathcal{K}(1 + |Dh|^2)^{\frac{3}{2}} \|Dh\| \|\mathbf{v}\|^2 \|\mathbf{w}\|.$$

This can be used in (27), together with $\|S\| \leq \mathcal{K}$ and $\|\nabla S\| \leq \mathcal{K}'$, to estimate the first term in (26) by

$$D_{\mathbf{v}}(\kappa_{\mathbf{v}}) \sqrt{1 + \|Dh\|^2} I(\mathbf{v}, \mathbf{v}) \leq (1 + |Dh|^2)^2 (\mathcal{K}' + 12\mathcal{K}^2 \|Dh\|).$$

The other two terms in (26) can be bounded, again using (23) and (24), by

$$\kappa_{\mathbf{v}} D_{\mathbf{v}} \left(\sqrt{1 + \|Dh\|^2} \right) I(\mathbf{v}, \mathbf{v}) \leq (1 + |Dh|^2)^2 \mathcal{K}^2 \|Dh\|$$

and

$$\kappa_{\mathbf{v}} \sqrt{1 + \|Dh\|^2} D_{\mathbf{v}}(I(\mathbf{v}, \mathbf{v})) \leq 2(1 + |Dh|^2)^2 \mathcal{K}^2 \|Dh\|.$$

Finally, we get the estimate

$$D_{\mathbf{v}}^3 h \leq (1 + |Dh|^2)^2 (\mathcal{K}' + 15\mathcal{K}^2 \|Dh\|). \quad (28)$$

We now seek to bound $\|Dh\|$. First observe that the sampling condition, $\epsilon \leq \frac{1}{2\mathcal{K}}$, provides a bound on the angle between the surface normal ν at p and q . To see this, consider an arc-length parametrized curve $\gamma : [0, \epsilon] \rightarrow M$ on the surface and its Gauss image, $\tilde{\gamma} = \nu \circ \gamma$, a curve on the unit sphere. The length of $\tilde{\gamma}$ is at least $\angle(\nu_p, \nu_q)$, i.e., the length of the minimizing geodesic joining ν_p and ν_q . The tangent vector of $\tilde{\gamma}$ is $S\gamma'$, and its length is therefore bounded by \mathcal{K} . Hence,

$$\angle(\nu_p, \nu_q) \leq \int_0^\epsilon \|S\gamma'(s)\| ds \leq \mathcal{K}\epsilon \leq \frac{1}{2}.$$

It follows that

$$\|Dh\| = \tan \angle(\nu_p, \nu_q) \leq \tan \frac{1}{2}.$$

Inserting this estimate into (25) and (28), we obtain (after generous rounding)

$$D_{\mathbf{v}}^2 h \leq 2\mathcal{K}^2 \quad \text{and} \quad D_{\mathbf{v}}^3 h \leq 2\mathcal{K}' + 14\mathcal{K}^2.$$

Finally, from (21), we infer that

$$|h(x, y)| \leq \mathcal{K}^2 d^3 \quad \text{and} \quad |h(x, y) - P(x, y)| \leq \frac{\mathcal{K}' + 7\mathcal{K}^2}{3} d^3.$$

The claims now follow from $d \leq \|\mathbf{e}\| \leq \epsilon$. \square

Proof of Lemma 7. Let \mathbf{e}_t , \mathbf{f}_t , and \mathbf{g}_t denote the tangential components of the \mathbf{e} , \mathbf{f} , and \mathbf{g} , respectively. By assumption, we have $(\mathbf{e}_t \times \mathbf{f}_t) \cdot \mathbf{n} > 0$ and $(\mathbf{e}_t \times \mathbf{g}_t) \cdot \mathbf{n} < 0$. The

tangential part of the discrete curvature vector is $(\mathbf{k}_e)_t = (\mathbf{J}_g \mathbf{e})_t + (\mathbf{J}_f \mathbf{f})_t$, where we deduce from (16) that

$$\begin{aligned} (\mathbf{J}_f \mathbf{e})_t &= \frac{\|\mathbf{e}\|^2 \mathbf{f}_t - (\mathbf{f} \cdot \mathbf{e}) \mathbf{e}_t}{\|\mathbf{e} \times \mathbf{f}\|} \\ &= \frac{\|\mathbf{e}_t \times \mathbf{f}_t\|}{\|\mathbf{e} \times \mathbf{f}\|} (-e_2, e_1, 0) - \frac{e_n^2 \mathbf{f}_t + e_n f_n \mathbf{e}_t}{\|\mathbf{e} \times \mathbf{f}\|}, \end{aligned}$$

and similarly

$$(\mathbf{J}_g \mathbf{e})_t = \frac{\|\mathbf{e}_t \times \mathbf{g}_t\|}{\|\mathbf{e} \times \mathbf{g}\|} (e_2, -e_1, 0) - \frac{e_n^2 \mathbf{g}_t + e_n g_n \mathbf{e}_t}{\|\mathbf{e} \times \mathbf{g}\|}.$$

Using Lemma 5 and the regularity condition (9) we get

$$\begin{aligned} \|\mathbf{e} \times \mathbf{f}\|^2 &= \|\mathbf{e}_t \times \mathbf{f}_t\|^2 + (e_n f_1 - e_1 f_n)^2 + (e_n f_2 - e_2 f_n)^2 \\ &\leq \|\mathbf{e}_t \times \mathbf{f}_t\|^2 + 8(\mathcal{K}\|\mathbf{e}\|\|\mathbf{f}\|\epsilon)^2 \\ &\leq \|\mathbf{e}_t \times \mathbf{f}_t\|^2 + 8\mathcal{K}^2 \rho^2 \epsilon^2 \|\mathbf{e} \times \mathbf{f}\|^2. \end{aligned}$$

Therefore,

$$1 \geq \frac{\|\mathbf{e}_t \times \mathbf{f}_t\|}{\|\mathbf{e} \times \mathbf{f}\|} \geq \frac{\|\mathbf{e}_t \times \mathbf{f}_t\|^2}{\|\mathbf{e} \times \mathbf{f}\|^2} \geq 1 - 8\mathcal{K}^2 \rho^2 \epsilon^2,$$

and analogously for \mathbf{g} . It follows that the two terms in $(\mathbf{J}_f \mathbf{e} + \mathbf{J}_g \mathbf{e})_t$ containing $(e_2, -e_1, 0)$ cancel out up to a term bounded by $(8\mathcal{K}^2 \rho^2) \epsilon^3$. Moreover, we observe that Lemma 5 and (9) yield

$$\begin{aligned} \frac{\|e_n^2 \mathbf{f}_t + e_n f_n \mathbf{e}_t\|}{\|\mathbf{e} \times \mathbf{f}\|} &\leq \frac{\mathcal{K}^2 \|\mathbf{e}\|^4 \|\mathbf{f}\| + \mathcal{K}^2 \|\mathbf{e}\|^3 \|\mathbf{f}\|^2}{\|\mathbf{e} \times \mathbf{f}\|} \\ &\leq 2\mathcal{K}^2 \rho \epsilon^3, \end{aligned}$$

and analogously for \mathbf{g} . Together, this yields

$$\|(\mathbf{J}_f \mathbf{e} + \mathbf{J}_g \mathbf{e})_t\| \leq (10\mathcal{K}^2 \rho^2) \epsilon^3,$$

proving the claim. \square